Research Article

Excellent cyclic performance of electrolytic MnO_2 in Li/MnO_2 rechargeable batteries

Zhen Cao[1,2] · Qizhen Xiao[1,2] · Gangtie Lei[2] · Zhaohui Li[2]

Received: 16 June 2019 / Accepted: 29 October 2019 / Published online: 2 November 2019

Abstract
The electrolytic MnO_2 particles with α·γ-MnO_2 is successfully prepared using one-step acid constant current electrodeposition method. Scanning electron microscope, N_2 adsorption/desorption method and X-ray diffraction are employed for the material characterization. Scanning electron microscope result shows that the diameter of MnO_2 particle is about 350–500 nm. A lot of mesoporous exist in the as-prepared MnO_2 particles, which exhibit high specific surface area and can provide significantly more electrochemical active sites for the redox reaction. The as-prepared MnO_2 particles as cathode in rechargeable Li/MnO_2 battery displays high discharge capacity of 202 mAh g^{-1} in the 1st cycle at a current density of 46 mA g^{-1}, and its discharge capacity retention ratio can achieve 82% over 100 cycles. The discharge capacities of the 100th cycle are 152, 127 and 114 mAh g^{-1} at different current densities of 151, 350 and 755 mA g^{-1}, respectively, indicating excellent rate capability. The promising electrochemical performance of α·γ-MnO_2 can make researchers focus again on using metal oxide as the cathode materials in the rechargeable Li-ion batteries.

Keywords Electrolytic MnO_2 · α·γ-MnO_2 · Cathode · Rechargeable Li-ion batteries

1 Introduction

The research and development of Li-ion secondary batteries have intensified because of its safety, high specific capacity and long cycle life. At present, $LiCoO_2$, $LiMn_2O_4$, and $LiFePO_4$ are dominating in the commercial cathode materials. In order to improve their power density and cycle stability, the novel derivatives of the above cathode materials, such as $LiNi_{0.8}Co_{0.2}O_2$ and $LiNi_{1/3}Co_{1/3}Mn_{1/3}O_2$ etc., are focused by researchers, which can be applied in plug-in/hybrid electric vehicles [1]. However, the commercial cathode materials in Li-ion batteries have some disadvantages such as high cost, toxicity and limited sources of Cobalt or Nickel, which restrict their development. Thus, it is urgent to develop the novel cathode materials in Li-ion secondary batteries with natural abundance, environmental friendliness, low cost and excellent electrochemical performance. The Li/MnO_2 battery has high discharge voltage (3 V), high energy density (230 Wh kg^{-1}) and long storage life. Electrolytic manganese dioxide (EMD) with high purity, low cost and strong electrochemical activity etc. is the critical component of the cathode material in commercial Li/MnO_2 primary battery [2–4], and it has a decisive influence on performance of cells. Furthermore, manganese oxide is inexpensive (less than 1% of the cost of Co) [5–7]. Developing and improving the cycle stability of EMD materials have been studied by researchers, but they show poor rechargeable ability [8–10].

Electronic supplementary material The online version of this article (https://doi.org/10.1007/s42452-019-1585-y) contains supplementary material, which is available to authorized users.

✉ Qizhen Xiao, qizhenxiao@yahoo.com | [1]School of Chemical and Environmental Engineering, Jiangsu University of Technology, Changzhou 213001, China. [2]Key Laboratory of Environmentally Friendly Chemistry and Applications of Ministry of Education, College of Chemistry, Xiangtan University, Xiangtan 411105, Hunan, China.

EMD is a multiphase material incorporating several polymorphs of MnO_2, and it possesses intergrowth, microtwinning, and phase mixture, which have been investigated [5, 11, 12]. The structure and morphology of EMD have been strongly influenced by various prepared parameters such as electrolyte, current density, electrodes (anode and cathode), bath temperature, current type and the pH of the electrolyte [4]. By decreasing the temperature and pH, the microtwinning EMD including α-MnO_2 and γ-MnO_2 has been prepared and extensively investigated as a cathode for Li-ion primary batteries [13]. The formation of α-MnO_2 in EMD at low pH is attributed to a template or structure-directing effect due to H_3O^+ [13].

As known to all, α-MnO_2 and γ-MnO_2 compounds with one-dimensional tunnel structure are favorable candidates for Li-ion secondary batteries. The structure of α-MnO_2 (Fig. 1a) is made up of double chains of edge-sharing octahedra which can share corners to form (2 × 2) and (1 × 1) channels, and the (2 × 2) channels have suitable size for the insertion/extraction of Li^+ [14]. Single-phase α-MnO_2 with high degree of crystallinity limits its use as insertion/extraction electrode in rechargeable Li-ion battery due to an instability of the large (2 × 2) channels of the α-MnO_2 framework to lithiation and an inability to electrochemically extract lithium below 3.8 V [5, 15]. γ-MnO_2 (Fig. 1b) with smaller (2 × 1) channels can provide greater stability than α-MnO_2, but the anisotropic expansion and contraction of the unit cell during lithium insertion/extraction cause structural damage and loss of capacity during cycling [16]. According to the study of Thackeray [17], the α-MnO_2 structure is inherently unstable. It could be stabilized by connecting to MnO_2 structures with smaller dimension channels to withstand the repeated insertion and extraction of lithium during cycling, thus the co-electrodeposited α·γ-MnO_2 exhibits good electrochemical performance. As depicted in Fig. 1c, it is expected that α·γ-MnO_2 composite with interconnected α-MnO_2 and γ-MnO_2 can make its structure more stable than single-phase α-MnO_2 or γ-MnO_2 during lithium insertion/extraction reactions [16].

At present, MnO_2 can be prepared by chemical and electrochemical methods, but it is difficult to prepare the intergrowth of α-MnO_2 and γ-MnO_2 with exact ratio of α-/γ-MnO_2 in the composite. In this paper, we introduce a facile electrodeposition method to prepare EMD particles on a large scale, and α·γ-MnO_2 composite with exact ratio can be obtained by controlling the electrolytic temperature and pH. The microstructure of α·γ-MnO_2 can composite the synergetic effects of α-MnO_2 and γ-MnO_2 and exhibit excellent cycle stability and rate capability. The promising electrochemical performance of α·γ-MnO_2 can make researchers focus again on using metal oxide as the cathode materials in the rechargeable Li-ion batteries.

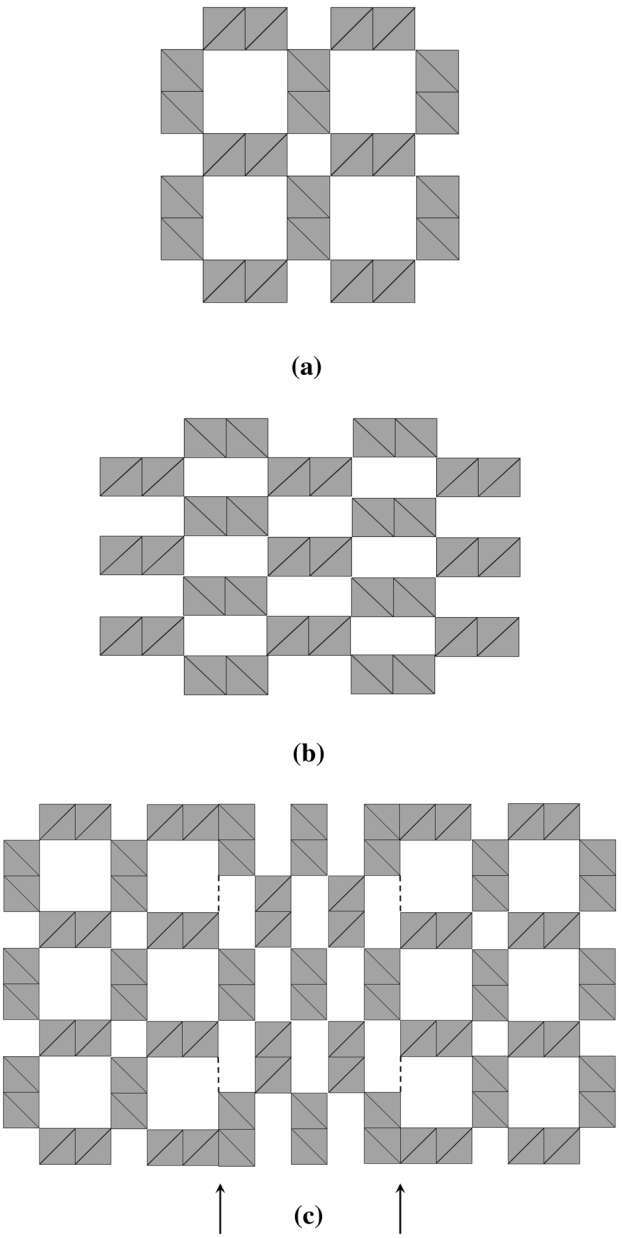

Fig. 1 The idealized MnO_2 structures for **a** α-MnO_2, **b** γ-MnO_2 and **c** the interconnected α·γ-MnO_2 composite

2 Experimental section

2.1 Synthesis and characterization of electrolytic MnO_2

All chemicals were analytical grade and were used without further purification. $MnSO_4·H_2O$ and concentrated sulfuric acid were supplied by Tianjin Chemical Reagent Company (P. R. China). Distilled water was used as solvent.

The EMD was prepared by constant current electrodeposition method in 5L electrolyte with current density of 300 A m^{-2} under 30 °C. Prior to electrodeposition, the lead plate with 10 cm × 13 cm was used as the working electrode after polishing and washing with detergent and distilled water. Copper plate was used as the counter electrode. The electrolyte was composed of 0.34 mol L^{-1} $MnSO_4$ and 0.47 mol L^{-1} H_2SO_4 (pH ≈ 0.03). The as-prepared EMD was purified by filtration, washing with distilled water and ethanol. The yield of as-prepared EMD was controlled to be 0.028 g cm^{-2} h^{-1}.

Scanning electron microscope (SEM) images were collected using JEOL JSM-6610LV microscope operated at the accelerating voltage of 30 kV. The phase structure of the as-prepared sample was identified using Rigaku D/max 2500 X-ray diffractometer (Cu, Kα radiation, λ = 1.5418 Å) at a voltage of 40 kV and a current of 250 mA with a scan rate of 0.02° s^{-1} (5° < 2θ < 90°) at room temperature. The BET (Brunauer–Emmett–Teller) surface area and the BJH (Barrett–Joyner–Halenda) pore distribution of the as-prepared sample were measured by the N_2 adsorption/desorption method (TriStarII3020, micromeritics, USA).

2.2 Electrochemical measurements

The electrochemical measurements were carried out using the CR 2016 coin-type cells. Test electrodes were prepared by mixing as-prepared EMD sample (80 wt%), acetylene black (10 wt%), and poly (vinylidene fluoride) (10 wt%). An amount of 3–5 mg of the mixture was coated on aluminum foil. The electrodes were dried at 60 °C in a vacuum drying oven for 24 h before use, and Li foil used as counter electrode. The coin-type cells were fitted together in a glovebox under an argon atmosphere. The electrolyte was a solution of 1 M $LiPF_6$ in ethylene carbonate (EC)-dimethyl carbonate (DMC) (volume ratio of 1:1). The constant current charge–discharge experiment was carried out on a NEWARE battery testing system (NEWARE BTS-5 V/5 mA) with a series of current densities of 46 mA g^{-1} (0.06 mA cm^{-2}), 151 mA g^{-1} (0.2 mA cm^{-2}), 350 mA g^{-1} (0.5 mA cm^{-2}) and 755 mA g^{-1} (1 mA cm^{-2}), the cells were charged and discharged between 4.2 and 1.8 V (vs. Li/Li^+). Cyclic voltammetry was carried out using a CHI660C electrochemical workstation (Shanghai, China) at a scan rate of 0.1 mV s^{-1}, with the operating voltage range consistent with the charge–discharge experiment. Electrochemical Impedance Spectroscopy (EIS) was carried out using a CHI660C Corrosion Electrochemical Measurement System (Shanghai, China) at a frequency range between 0.01 and 10^5 Hz.

3 Results and discussion

Figure 2 shows the typical SEM images of as-prepared EMD material. The uniform EMD particles can be found in Fig. 2a, the diameters of EMD particles are about 350–500 nm. As shown in Fig. 2b, part of EMD particles are aggregated with each other which can be ascribed to their high surface energy during prepared process. To our knowledge, the EMD not only provides the enhancement in the Li^+ effective insertion pathways, but also enhances diffusion kinetics due to the increase of the specific surface area, which can improve the rate capacity of electrode.

The N_2 adsorption/desorption isotherms and the pore size distribution (inset) of as-prepared EMD material are presented in Fig. 3. The BET surface area of the EMD material is 66 m^2 g^{-1}, which can be calculated from N_2 adsorption. As shown in Fig. 3, the adsorption/desorption isotherms are identified as type II, which is characteristic of

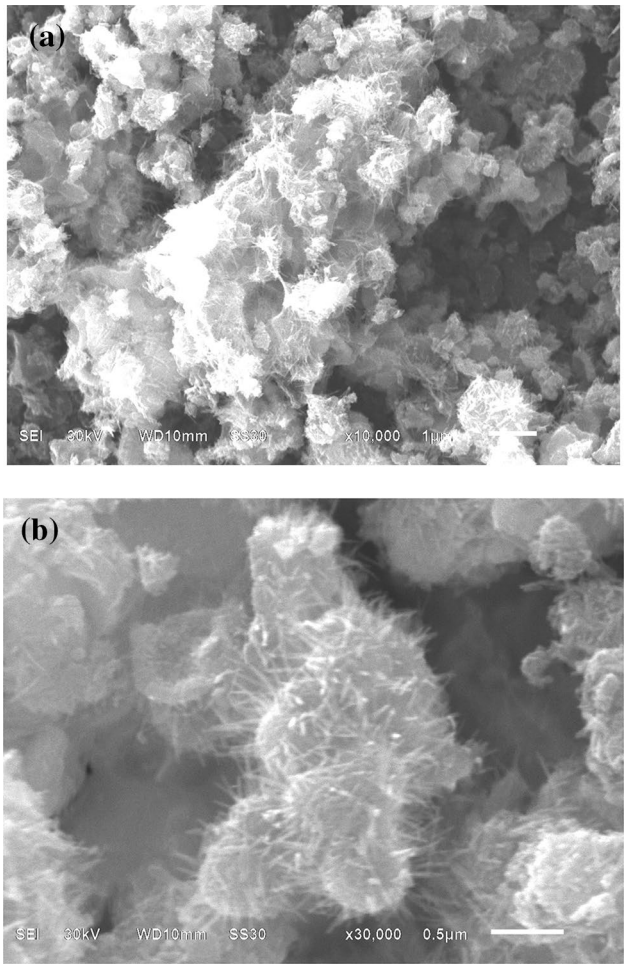

Fig. 2 **a** SEM image of as-prepared EMD material, **b** the higher magnification SEM image of as-prepared EMD material

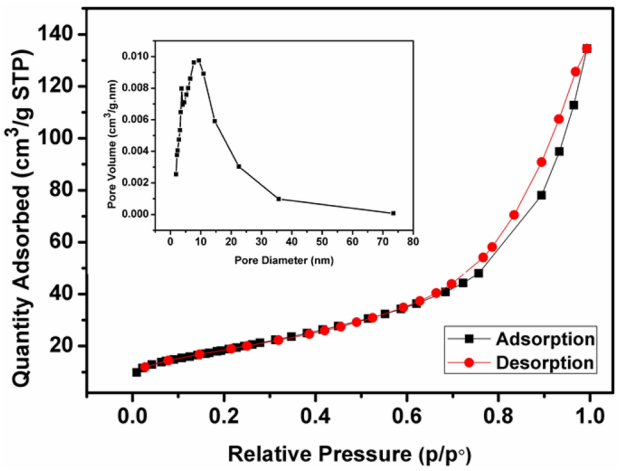

Fig. 3 N_2 adsorption/desorption isotherms and pore size distribution (inset) of as-prepared EMD material

mesoporous materials [18–20]. It can be known from the inset of Fig. 3 that the pore size is centered at 10 nm with a narrow distribution. Mesoporous structure is beneficial for the migration of Li^+ and transfer of electron, and corresponds to the superior electrochemical performance of the MnO_2 samples [19, 20]. In a word, mesoporous structure and high specific surface area can further improve the electrochemical performance of the EMD.

Figure 4 shows the XRD pattern and the fitting result of as-prepared EMD material. All diffraction peaks can be indexed to α-MnO_2 (JCPDS NO. 72-1982) and γ-MnO_2 (JCPDS NO. 43-1455), which are in good agreement with the standard values, indicating that the intergrowth of two crystalline can be produced by controlling electrolytic process. The fitting result using the software of Jade 6.0 matches well with the tested diffraction peak, indicating a better fitting. The mass fraction of α-MnO_2 in the composite can be calculated to be 55 wt%. The result shows that it is simple and facile to prepare the EMD with intergrowth of α·γ-MnO_2 compared with the chemically-produced material [11].

Reversibility of as-prepared EMD cathode is investigated by cyclic voltammetry. As shown in Fig. 5, the reduction peak (R) of the 2nd cycle is significantly different from the 1st cycle. The potential of reduction peak shifts from 2.53 to 2.61 V, and current of reduction peak decreases significantly, indicating that an irreversible phase conversion can occur during the first cycle. The oxidation peak (O) gradually shifts to high potential, indicating that the extraction of Li^+ is becoming difficult with the increasing reduction depth. Furthermore, the reduction peak slightly shifts to opposite direction from 3rd to 5th cycle, reaching 2.53 V in the 5th cycle. The peak potential difference between reduction and oxidation gradually stabilizes during cycling. This result suggests that an irreversible phase conversion and the electrochemical activation can be gradually completed in several cycles. This result is in accordance with the cycle performance.

Figure 6a shows the charge–discharge behaviors of as-prepared EMD cathode in rechargeable Li/MnO_2 battery at current density of 46 mA g^{-1}. From Fig. 6a, the first discharge curve of the EMD cathode shows a flat plateau in the voltage range between 3.0 and 2.4 V, and the discharge capacity reaches 202 mAh g^{-1}, indicating that a desirable lithium inserted amount can be obtained at the low current density. This value is much higher than that of the related materials [21]. The shapes of charge–discharge curves are analogous. The discharge capacity of EMD [20] cathode still delivers 166 mAh g^{-1} at the 100th cycle. The capacity retention ratio is 99% compared with 2nd cycle

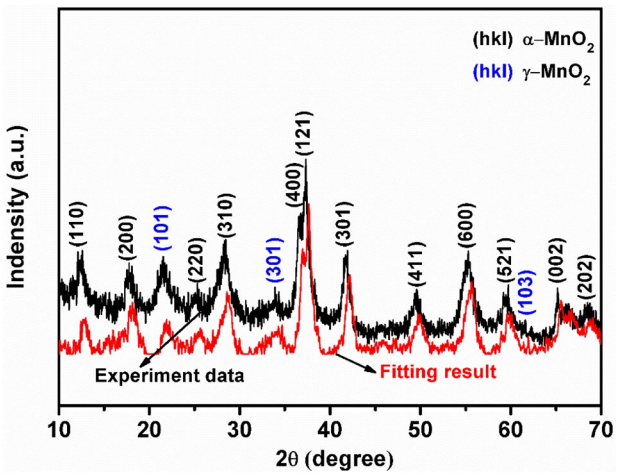

Fig. 4 XRD pattern and the fitting result of as-prepared EMD material

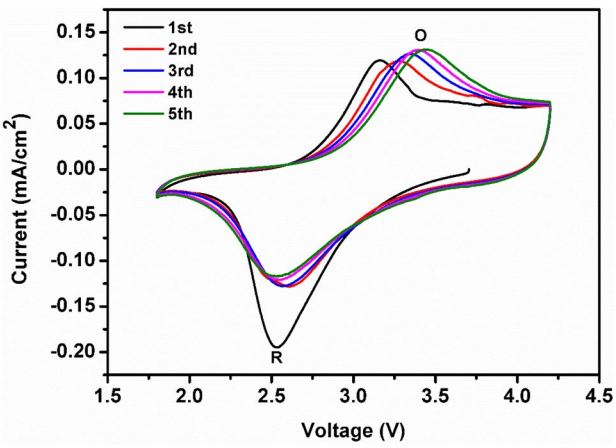

Fig. 5 Cyclic voltammogram of as-prepared EMD cathode at the scan rate of 0.1 mV s^{-1} between 4.2 and 1.8 V

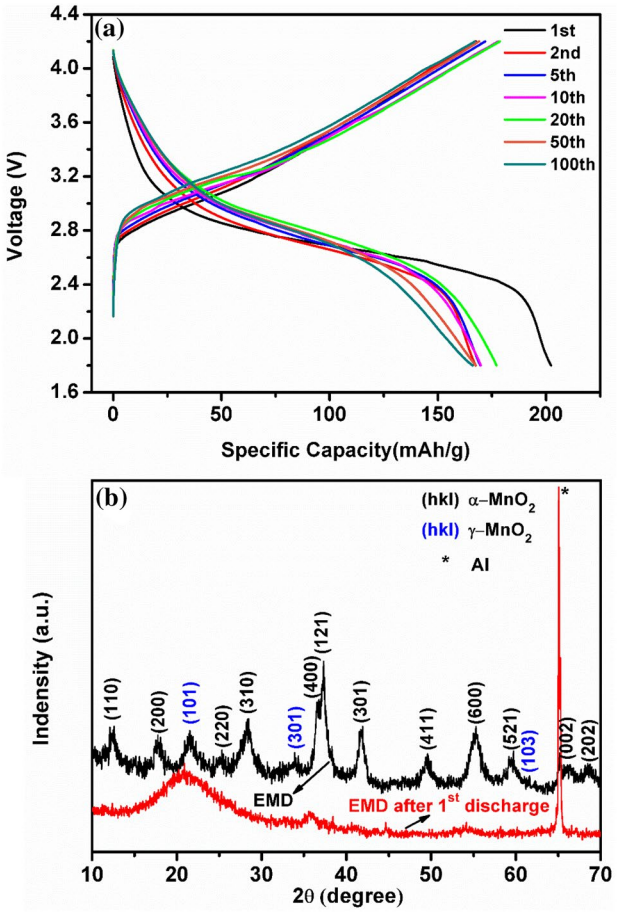

Fig. 6 **a** Charge–discharge curves of as-prepared EMD cathode at 1st, 2nd, 5th, 10th, 20th, 50th and 100th cycles, **b** XRD pattern of as-prepared EMD and EMD cathode after 1st discharge

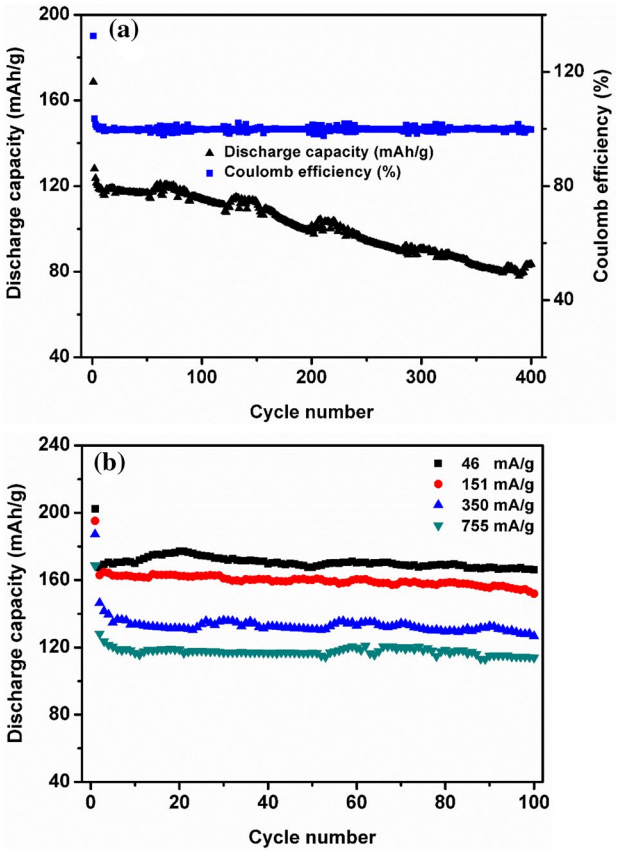

Fig. 7 **a** The cycle performance of as-prepared EMD cathode at current density of 755 mA g^{-1}, **b** the rate capability of as-prepared EMD cathode at different current densities of 46, 151, 350 and 755 mA g^{-1}

(167 mAh g^{-1}), exhibiting the excellent cycle stability. It can be seen that the discharge voltage plateau slightly increases from 1st to 5th cycle, which can be stable after 5 cycles. The result is in accordance with cyclic voltammetry, indicating that the irreversible phase conversion occurs in the first cycle and gradually finishes in several cycles. Figure 6b shows the XRD pattern of as-prepared EMD and EMD cathode after 1st discharge. From Fig. 6b, there is no obvious Li_xMnO_2 peak after 1st discharge and the structure of α·γ-MnO_2 may be maintained, but the peak at 21.06° belonging to γ-MnO_2 become wider and shifts to the left, indicating that the interplanar spacing become larger, which may be caused by the contraction/deformation of the large (2 × 2) channels of the α-MnO_2 or the expansion of the (2 × 1) channels of the γ-MnO_2 after insertion of Li^+. During the first few cycles, the deformed channels may make it difficult to remove lithium, leading to the gradual rise of the charging platform and capacity fading. After the first few cycles, the stable microstructure of α·γ-MnO_2 can make better charge and discharge efficiency and cycle performance in the subsequent cycle, which is consistent with the charge–discharge curves and CVs.

Figure 7 shows the cycle performance and rate capability of as-prepared EMD cathode between 4.2 and 1.8 V. From Fig. 7a, the discharge capacity of EMD cathode retains 84 mAh g^{-1} over 400 cycles with high current density of 755 mA g^{-1} (1 mA cm^{-2}). The capacity retention ratio is 66% after 400 cycles compared with 2nd cycle (128 mAh g^{-1}). According to research of Haibo Tan [21], the capacity retention ratio of EMD materials at the 100th cycle is 54% compared with 2nd cycle (0.1 mA cm^{-2}). The capacity loss is primarily attributed to the crystal structure transformation by capture of lithium ions during cycling [21, 22]. As far as we know, the key of improving electrochemical performance of EMD is to control the microstructure of the intergrowth of α-MnO_2 and γ-MnO_2. The interconnected α-MnO_2 and γ-MnO_2 can make its structure more stable during lithium insertion/extraction reactions. To further evaluate the rate capability of the EMD cathode, current densities from 46 to as high as 755 mA g^{-1} are applied to the half-cells. Figure 7b shows the discharge

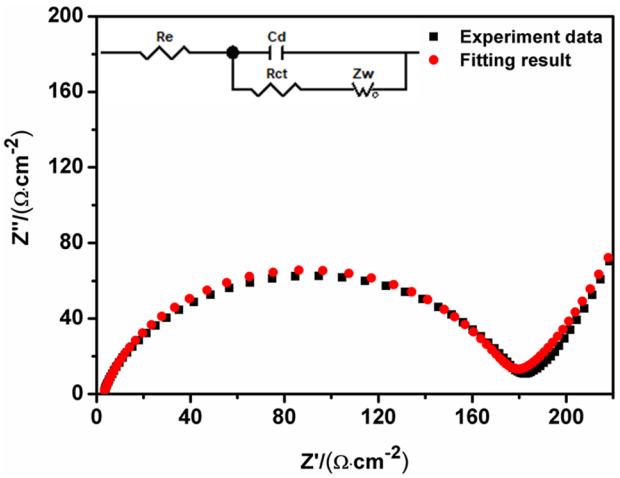

Fig. 8 Nyquist plots of the EMD cathode and the corresponding simulation result (Inset: equivalent circuit)

capacities at four different current densities. The reversible capacities retains 166, 152, 127 and 114 mAh g^{-1} of 100th cycle at current densities of 46, 151, 350 and 755 mA g^{-1}, and the reversible capacity retention ratios of 100th cycle are 82, 83, 68 and 68% compared with 1st cycle, respectively. The results suggest that the capacities at each current density are quite stable without notable fading. The excellent rate capability can result from high surface area, mesoporous structure [19] of the EMD cathode and the stable microstructure of α·γ-MnO_2 [16].

To investigate more information about the kinetic behavior of the Li^+ insertion process in the as-prepared EMD cathode, an electrochemical impedance spectroscopy (EIS) test was performed. Figure 8 is Nyquist plots of the EMD cathode and the corresponding simulation result. Inset is the equivalent circuit. The Nyquist plots consist of one semicircle in the high frequency region, which is attributed to the charge transfer impedance (R_{ct}), and an inclined line in the low frequency region is related to Warburg impedance (Z_w). The R_{ct} and Z_w of the as-prepared EMD cathode is 142 and 143 Ω cm^{-2}, respectively. The low R_{ct} and Z_w imply that the as-prepared EMD has the low Li^+ diffusion activation energy and high diffusion rate of Li^+, resulting in the fast redox reaction.

4 Conclusions

In summary, EMD (α·γ-MnO_2) with intergrowth of α-MnO_2 and γ-MnO_2 is prepared by constant current electrodeposition method. The prepared method is simple, which is suitable for large-scale application. The intergrowth of α-MnO_2 and γ-MnO_2 with interconnected microstructure can inhibit their crystal structure transformation during Li-ion insertion/extraction reactions. The EMD with mesoporous structure has high specific surface area, which can effectively improve the rate capability. In a word, the EMD delivers high initial specific capacity, excellent cycle stability and rate capability, which can be attributed to the stable microstructure of α·γ-MnO_2, high specific surface area, mesoporous structure and smaller particles.

Funding This study was funded by the national natural science foundation of China (21174119), the Scientific Research Foundation for the Returned Overseas Chinese Scholars, State Education Ministry, and the Natural Science Founding of Hunan Provincial (2018JJ2386).

Compliance with ethical standards

Conflict of interest The authors declare that they have no conflict of interest.

References

1. Tai Z, Subramaniyam CM, Chou SL, Chen L, Liu HK, Dou SX (2017) Few atomic layered lithium cathode materials to achieve ultrahigh rate capability in lithium-ion batteries. Adv Mater 29:1700605
2. Yun YS, Kim JM, Park HH, Lee J, Huh YS, Jin H (2013) Free-standing heterogeneous hybrid papers based on mesoporous γ-MnO2 particles and carbon nanotubes for lithium-ion battery anodes. J Power Sources 244:747
3. Sarkar D, Khan GG, Singh AK, Mandal K (2013) High-performance pseudocapacitor electrodes based on α-Fe2O3/MnO2 core–shell nanowire heterostructure arrays. J Phys Chem C 117:15523
4. Biswal A, Tripathy BC, Sanjay K, Subbaiah T, Minakshi M (2015) Electrolytic manganese dioxide (EMD): a perspective on worldwide production, reserves and its role in electrochemistry. RSC Adv 5:58255
5. Johnson CS, Mansuetto MF, Thackeray MM, Shao-Horn Y, Hackney SA (1997) Stabilized alpha-MnO2 electrodes for rechargeable 3 V lithium batteries. J Electrochem Soc 144:2279
6. Liu Z, Wang WL, Liu X, Wu M, Li D, Zeng Z (2004) Hydrothermal synthesis of nanostructured spinel lithium manganese oxide. J Solid State Chem 177:1585
7. Johnson CS (2007) Development and utility of manganese oxides as cathodes in lithium batteries. J Power Sources 165:559
8. Dampier FW (1974) The cathodic behavior of CuS, MoO3, and MnO2 in lithium cells. J Electrochem Soc 121:656
9. Pistoia G (1982) Some restatements on the nature and behavior of MnO2 for Li batteries. J Electrochem Soc 129:1861
10. Nohma T, Saito T, Furukawa N, Ikeda H (1989) Manganese oxides for a lithium secondary battery—composite dimensional manganese oxide (CDMO). J Power Sources 26:389
11. Chabre Y, Pannetier J (1995) Structural and electrochemical properties of the proton/γ-MnO2 system. Prog Solid State Chem 23:1
12. Balachandran D, Morgan D, Ceder G, Walle AVD (2003) First-principles study of the structure of stoichiometric and Mn-deficient MnO2. J Solid State Chem 173:462
13. Adelkhani H, Ghaemi M (2009) Influence of the solution pH on the nanostructural, and electrochemical performance of electrolytic manganese dioxide. J Alloys Compd 481:446

14. Hill LI, Verbaere A, Guyomard D (2003) MnO2 (α-, β-, γ-) compounds prepared by hydrothermal-electrochemical synthesis: characterization, morphology, and lithium insertion behavior. J Power Sources 119–121:226
15. Yuan G, Dahn JR (1996) Synthesis and characterization of Li1 + x Mn2 – x O4 for Li-ion battery applications. J Electrochem Soc 143:100
16. Wells AF (1975) Structural inorganic chemistry, 4th edn. Clarendon Press, Wotton-under-Edge
17. Thackeray MM (1997) Manganese oxides for lithium batteries. Prog Solid State Chem 25:1
18. Vinu A, Sawant DP, Ariga K, Hartmann M, Halligudi SB (2005) Benzylation of benzene and other aromatics by benzyl chloride over mesoporous AlSBA-15 catalysts. Microporous Mesoporous Mater 80:195
19. Sun Y, Wang S, Dai Y, Lei X (2015) Electrochemical characterization of nano V, Ti doped MnO_2 in primary lithium manganese dioxide batteries with high rate. Funct Mater Lett 9:1650005
20. Moulai F, Cherchour N, Messaoudi B, Zerroual L (2016) Electrosynthesis and characterization of nanostructured MnO2 deposited on stainless steel electrode: a comparative study with commercial EMD. Ionics 23:1
21. Tan H, Wang S, Lei X (2015) New insights for the cyclic performance of Li/MnO2 batteries using a simple electrochemical process. J Electrochem Soc 162:A448
22. Shao-Horn Y, Hackney SA, Cornilsen BC (1997) Structural characterization of heat-treated electrolytic manganese dioxide and topotactic transformation of discharge products in the Li-MnO2 cells. J Electrochem Soc 144:3147